

Operator-induced structural variable selection for identifying materials genes

Shengbin Ye ^{*1}, Thomas P. Senftle ^{†2}, Meng Li ^{‡1}

¹Department of Statistics, Rice University, Houston, TX 77005

²Department of Chemical and Biomolecular Engineering, Rice University, Houston, TX 77005

November 23, 2021

Abstract

In the emerging field of materials informatics, a fundamental task is to identify physicochemically meaningful descriptors, or materials genes, which are engineered from primary variables and a set of elementary algebraic operators through compositions. Standard practice directly analyzes the high-dimensional candidate predictor space in a linear model; statistical analyses are then substantially hampered by the daunting challenge posed by the astronomically large number of correlated predictors with limited sample size. We formulate this problem as variable selection with operator-induced structure (OIS), and propose a new method to achieve unconventional dimension reduction by utilizing the geometry embedded in OIS. Although the model remains linear, we iterate nonparametric variable selection for effective dimension reduction. This enables variable selection based on *ab initio* primary variables, leading to a method that is orders of magnitude faster than existing methods, with improved accuracy. An OIS screening property for variable selection with OIS is introduced; interestingly, finite sample assessment indicates that the employed Bayesian Additive Regression Trees (BART)-based variable selection method enjoys this property under the simulation settings. Numerical studies show the superiority of the proposed method, which continues to exhibit robust performance when the dimension of engineered features is out of reach of existing methods. Our analysis to single-atom catalysis identifies physical descriptors that explain the binding energy of metal-support pairs with high explanatory power, leading to interpretable insights to guide the prevention of a notorious problem called sintering and aid catalysis design.

Keywords: BART; Bayesian nonparametrics; feature engineering; materials genomes; non-parametric dimension reduction

^{*}sy53@rice.edu

[†]tsenftle@rice.edu

[‡]meng@rice.edu

1 Introduction

The Materials Genome Initiative set up by the White House is a large-scale effort concerning the utilization of computational tools to accelerate the pace of discovery and deployment of advanced material systems. Since its inception in 2011, there has been a surge of interest in data-driven materials design and understanding (Zhong et al., 2020; Hart et al., 2021; Keith et al., 2021; Lin et al., 2021; Liu et al., 2021b; Miller et al., 2021). In this nascent area called materials informatics, computational methods that account for physical and chemical mechanisms of a material system play a central role in aiding, augmenting, or even replacing time-consuming trial and error experimentation. A fundamental task is to identify physicochemically meaningful *descriptors*, or *materials genes* (Ghiringhelli et al., 2015; Foppa et al., 2021). These descriptors, for example, are key to modelling single-atom catalysis and finding or developing more efficient catalytically active materials. Unlike existing variable selection problems, the high-dimensional predictors in materials genome possess strong inherent structure in that they are engineered using a set of primary features $\mathbf{X} = (\mathbf{x}_1, \dots, \mathbf{x}_p)$ and *compositions of operators* \mathcal{O} .

Suppose the response vector \mathbf{y} measures the material property of interest, and the primary predictor matrix $\mathbf{X} = (\mathbf{x}_1, \dots, \mathbf{x}_p)$ collects physical or chemical properties of the materials such as atomic radii, ionization energies, etc. Then the space of engineered predictors is $\mathcal{O}^{(M)}(\mathbf{X})$, which consists of nonlinear predictors with explicit functional form resulting from M -order compositions of operators \mathcal{O} on the primary features \mathbf{X} . For example, some commonly used operators in materials genome are

$$\mathcal{O} = \{+, -, \times, /, | - |, I, \exp, \log, |\cdot|, \sqrt{\cdot}, ^{-1}, ^2, \sin(\pi \cdot), \cos(\pi \cdot)\}, \quad (1)$$

and an example of a descriptor may be $f(\mathbf{X}) = \{\exp(\mathbf{x}_1) - \exp(\mathbf{x}_2)\}^2$ which belongs to $\mathcal{O}^{(3)}(\mathbf{X})$. We refer to this distinctive geometry encoded in $\mathcal{O}^{(M)}(\mathbf{X})$ as variable selection with *operator-induced structure* (OIS). The aforementioned descriptors in materials genome are thus the predictors in a linear model with OIS. Henceforth, we will use *descriptor*

selection and variable selection in the presence of OIS interchangeably.

The geometry of OIS defined by operators \mathcal{O} and high-order compositions induces high correlation and ultra-high dimension of the feature space. For example, $\mathcal{O}^{(3)}(\mathbf{X})$ with the operator in (1) and $p = 20$ produces an astronomically large number of predictors at the scale of 10^{11} , and this cardinality increases double exponentially with M and the number of binary operators using p as the base constant. In our real data application, the number of primary features is $p = 59$ and enumerating $\mathcal{O}^{(3)}(\mathbf{X})$ gives 1.01×10^{17} predictors, more than the total number of cells in human body which is on the order of 10^{13} (Sender et al., 2016). These predictors are highly correlated as a result of iteratively applying unary operators. Materials genomes are an analogue concept to genomes, but the dimension of predictors and inherent strong correlation in materials genome-wide association studies, or *materials GWAS*, pose unprecedented challenges to statistical analysis.

In this article, we develop a powerful method for materials GWAS in which we effectively identify materials genes that are associated with the response of interest. While the model is assumed to be linear, we employ nonparametric variable selection to achieve dimension reduction, a novel strategy that we call “parametrics assisted by nonparametrics”, or PAN. We iterate the nonparametric method in light of the composition structure in OIS. There has been an extensive literature on variable selection in statistics over the past three decades; however, existing methods may not account for the geometry defined in OIS. A related literature on heredity constraints has been focused on interactions of primary variables (Ravikumar et al., 2009; Choi et al., 2010; Radchenko and James, 2010; Bien et al., 2013; She et al., 2018), in which the operator set \mathcal{O} only consists of the multiplication and the identity operator, and the order of composition is typically as limited as two. In contrast, OIS in materials genome is defined by considerably more operators and higher-order compositions, generating a massive set of predictors with extraordinary capacity yet at a scale that renders existing methods computationally infeasible.

The key idea in PAN is to apply a small set of operators and immediately identify the relevant descriptors (or operators and variables) in a nonparametric context before

constructing more complex descriptors, in an iterative fashion instead of a one-shot approach. To ensure selection accuracy under OIS, we introduce and discuss an *OIS screening property* for nonparametric variable selection that is unique to OIS, in that a nonparametric method needs to select the correct model under ambiguity.

While PAN complements a large class of nonparametric methods, we focus on the Bayesian additive regression tree method (BART; Chipman et al. (2010)) partly because of its excellent performance in a variety of applications. This leads to a new method called iterative BART, or iBART, for variable selection in the presence of OIS. iBART reduces the size of the working descriptor space significantly, mitigating collinearity in the process, and the use of nonparametric variable selection accounts for structural model misspecification in intermediate variable selection steps. Interestingly, we find that a BART-based variable selection method (Bleich et al., 2014) tends to achieve the OIS screening property at least under the simulation settings—a phenomenon that has not been studied in the literature. Simulations in Section 3 show superior performance of iBART relative to existing methods. In the application to single-atom catalysis in Section 4, iBART identifies physical descriptors that explain the binding energy of metal-support pairs with high explanatory power, leading to interpretable insights to guide the prevention of a notorious problem called sintering.

1.1 Related work

Descriptor selection has attracted growing attention in materials science. Several methods have been recently proposed, building on a *one-shot* descriptor generation and selection scheme followed by modern statistical variable selection methods (O’Connor et al., 2018; Ouyang et al., 2018; Liu et al., 2020). In particular, they first construct descriptors by applying operators iteratively M times on the primary feature space $\mathbf{X}_0 \equiv \mathbf{X} = (\mathbf{x}_1, \dots, \mathbf{x}_p) \in \mathbb{R}^{n \times p}$ to construct a ultra-high dimensional descriptor space $\mathbf{X}_M \equiv \mathcal{O}^{(M)}(\mathbf{X}_0)$ of $O(p^{2^M})$ descriptors, assuming binary operators are used in each iteration. Then variants of generic statistical methods are adopted to select variables from \mathbf{X}_M . Along this line, the method SISSO (Sure Independence Screening and Sparsifying Operator) proposed by

Ouyang et al. (2018) builds on Sure Independence Screening, or SIS (Fan and Lv, 2008), O’Connor et al. (2018) uses LASSO (Tibshirani, 1996), and Liu et al. (2020) adopts Bayesian variable selection methods.

SISSO is widely perceived as one of the most popular methods for materials genome. It utilizes SIS to screen out P descriptors, from which the single best descriptor is selected using an ℓ_0 -penalized regression. If a total of k descriptors are desired, this process will be iterated for k times yielding k sets of SIS-selected descriptors, followed by an ℓ_0 -penalized regression to select the best k descriptors from all the SIS-selected descriptors. Note that in each iteration, SIS is employed to screen out P descriptors from the remaining descriptor set with an updated response vector given by its least squares residuals projected onto the space spanned by previously SIS-selected descriptors. Users must define the composition complexity of the descriptors through M , i.e., the order of compositions of operators. In a typical application of SISSO, the order of composition M is no greater than 3, the number of candidate descriptors in each SIS iteration is less than 100, and the number of descriptors k is no larger than 5 (Ouyang et al., 2018). Note that selecting 5 descriptors with 100 SIS-selected descriptors in each iteration amounts to fitting at most $\binom{500}{5} \approx 2.6 \times 10^{11}$ different regressions, which is computationally intensive.

A major drawback of these one-shot descriptor construction procedures is the introduction of a highly correlated and ultra-high dimensional descriptor space $\mathbf{X}_M = \mathcal{O}^{(M)}(\mathbf{X}_0)$. High correlation often hampers the performance of a variable selection method, and the ultra-high dimensional descriptor space with large p , as common in modern applications, can make it computationally prohibitive for such methods. In practice, these methods often resort to ad hoc adaptation or sacrifice the complexity level of candidate descriptors.

Another thread of work is the well-developed *automatic feature engineering* in machine learning, which aims to generate complex features from any given set of constructor functions adaptively (Markovitch and Rosenstein, 2002; Dor and Reich, 2012; Feurer et al., 2015; Khurana et al., 2018). However, the overwhelming focus of this literature is on increasing the predictive power of the primary variables \mathbf{X} . We instead focus on discovering the

underlying functional relationship between the response and the predictors and revealing data-driven insights into the underlying physics for materials design. In addition, the sample size in materials genome is typically limited, hampering the use of machine learning methods that rely on large training data.

In statistics, transformations have been commonly used to expand the predictor space, including polynomials, logarithmic, and power transformations, and the previously noted interactions. The induced feature spaces from these elementary transformations are often overly simple to capture the intricate dynamics of the response in materials genome, particularly compared to high-order compositions of a larger operator set. There has been a rich literature on nonparametric variable selection, but descriptor selection relies on a linear model with feature engineering that favorably points to interpretable insights for domain experts as the functional forms of selected variables are explicitly given and the feature space could be composed using domain-related knowledge. The nonparametric module in PAN only serves as a dimension reduction tool, and its performance crucially depends on the OIS screening property that is unique to descriptor selection. Overall, materials GWAS may play an analogous role that GWAS have played in motivating new statistical methods and concepts, and to the best of knowledge, the present article is the first statistical work on this topic.

2 The OIS framework

2.1 Operator-induced structural model

We begin with a standard ultra-dimensional linear regression model

$$\mathbf{y} = \beta_0 + \beta_1 \mathbf{x}_1 + \cdots + \beta_{p^*} \mathbf{x}_{p^*} + \boldsymbol{\varepsilon}, \quad (2)$$

where $\boldsymbol{\varepsilon} \sim \mathcal{N}_n(\mathbf{0}, \sigma^2 \mathbf{I})$ is a Gaussian noise vector, and regression coefficients $\boldsymbol{\beta}$ are sparse. The dimension of predictors p^* is ultra-high, at the materials GWAS scale that typically

exceeds the maximum size of vectors allowed by a modern personal computer, while the sample size n is on the order of tens. This seemingly ultra-dimensional descriptor space obeys an operator-induced structure (OIS). In particular, the predictors $\mathbf{x}_1, \dots, \mathbf{x}_{p^*}$ in (2), or *descriptors*, are generated by applying operators in \mathcal{O} iteratively M times on a primary feature space $\mathbf{X}_0 = (\mathbf{x}_1, \dots, \mathbf{x}_p) \in \mathbb{R}^{n \times p}$, i.e.,

$$(\mathbf{x}_1, \dots, \mathbf{x}_{p^*}) \equiv \mathbf{X}_M = \mathcal{O}^{(M)}(\mathbf{X}_0) = \mathcal{O} \circ \mathcal{O}^{(M-1)}(\mathbf{X}_0) = \underbrace{\mathcal{O} \circ \dots \circ \mathcal{O}}_{M \text{ times}}(\mathbf{X}_0), \quad (3)$$

where $\mathbf{X}_M = \mathcal{O}^{(M)}(\mathbf{X}_0)$ denotes M -composition of all operators in \mathcal{O} on \mathbf{X}_0 and can be defined iteratively as above. The operator set \mathcal{O} is user-defined; for concreteness, we focus on the common example given in (1), unless stated otherwise.

We adopt the following convention. Evaluation of operators on vectors is defined to be entry-wise, e.g., $\mathbf{x}_1^2 = (x_{1,1}^2, \dots, x_{n,1}^2)^T$ and $\mathbf{x}_1 + \mathbf{x}_2 = (x_{1,1} + x_{1,2}, \dots, x_{n,1} + x_{n,2})^T$. There may exist redundant descriptors following (3). For example, the two descriptors $\text{square}(\mathbf{x}) = \mathbf{x}^2$ and $\text{multiplication}(\mathbf{x}, \mathbf{x}) = \mathbf{x} \times \mathbf{x}$ are equivalent. Throughout this article, redundant descriptors are excluded from \mathbf{X}_M in (3), which can be easily achieved in practice by identifying and removing perfectly correlated descriptors.

We hereafter refer to the linear regression model in (2) along with the operator-induced structure (OIS) in (3) as the OIS model. The regression coefficients in the OIS model are assumed to be extremely sparse, and it is useful to recast the OIS model using predictors with nonzero coefficients. To this end, we define *M -composition- \mathcal{S} -variate descriptor*, where $M \in \mathbb{N}$ is any positive integer and $\mathcal{S} \subseteq [p] = \{1, \dots, p\}$ is any subset of predictor indices.

Definition 2.1. We define $f^{M,\mathcal{S}}(\mathbf{X})$ to be an M -composition- \mathcal{S} -variate descriptor if it is constructed via M compositions of operators on the primary features \mathbf{X}_S :

$$f^{M,\mathcal{S}}(\mathbf{X}) = f^{M,\mathcal{S}}(\mathbf{X}_S) = o^{(M)}(\mathbf{X}_S) = o_M \circ f^{(M-1),\mathcal{S}}(\mathbf{X}_S) = o_M \circ o_{M-1} \circ \dots \circ o_1(\mathbf{X}_S),$$

where $o_m \in \mathcal{O}$ is the m th composition operator(s) for $1 \leq m \leq M$, and $f^{1,\mathcal{S}}(\mathbf{X}_S), \dots, f^{(M-1),\mathcal{S}}(\mathbf{X}_S)$

are the necessary lower composition complexity descriptors for constructing the descriptor $f^{M,\mathcal{S}}(\mathbf{X}_{\mathcal{S}})$. Note that if the m th composition operator is a binary operator, there may exist two $(m-1)$ th composition operators but we suppress the notation here for simplicity.

Then the OIS model in (3) can be rewritten into

$$y_i = \beta_0 + \sum_{k=1}^K f_k^{M,\mathcal{S}}(x_{i,1}, \dots, x_{i,p})\beta_k + \varepsilon_i, \quad i = 1, \dots, n, \quad (4)$$

where M denotes the highest order of operator compositions and K denotes the number of additive descriptors. We now refer to (4) as an M -composition- \mathcal{S} -variate OIS model. Although the notation in (4) seems to suggest that all K descriptors are M -composition descriptors, the composition complexity of the descriptors need not be the same. For instance, one can construct an equivalent M -composition- \mathcal{S} -variate descriptor $f^{M,\mathcal{S}}$ from a m -composition- \mathcal{S} -variate descriptor $f^{m,\mathcal{S}}$, where $m \leq M$, by applying the identity operator I for $M-m$ times on $f^{m,\mathcal{S}}$: $f^{M,\mathcal{S}}(\mathbf{X}) = I^{(M-m)} \circ f^{m,\mathcal{S}}(\mathbf{X}) = f^{m,\mathcal{S}}(\mathbf{X})$. The usage of the identity operator I thus does not contribute to the composition complexity of a descriptor in a meaningful way. Hence, we define the notion of nontrivial composition complexity below to describe the “true” composition complexity of a descriptor.

Definition 2.2 (Nontrivial composition complexity). *The nontrivial composition complexity of an M -composition- \mathcal{S} -variate descriptor $f^{(M,\mathcal{S})}(\mathbf{X})$ is the smallest $k' \in \{1, \dots, M\}$ such that $f^{M,\mathcal{S}}(\mathbf{X}) = I^{(M-k')} \circ f^{k',\mathcal{S}}(\mathbf{X})$ for some $f^{k',\mathcal{S}}(\mathbf{X})$.*

We next use a toy example to illustrate descriptors, OIS, and the challenge posed by descriptor selection. Suppose that the true data generating model is

$$\begin{aligned} \mathbf{y} &= \beta_0 + \beta_1 f_1^{M_1, \mathcal{S}_1}(\mathbf{X}_0) + \beta_2 f_2^{M_2, \mathcal{S}_2}(\mathbf{X}_0) + \varepsilon \\ &= \beta_0 + \beta_1 \{\exp(\mathbf{x}_1) - \exp(\mathbf{x}_2)\}^2 + \beta_2 \sin(\pi \mathbf{x}_3 \mathbf{x}_4) + \varepsilon. \end{aligned} \quad (5)$$

Here the first term $\{\exp(\mathbf{x}_1) - \exp(\mathbf{x}_2)\}^2$ is a 3-composition- $\{1, 2\}$ -variate descriptor and the second term $\sin(\pi \mathbf{x}_3 \mathbf{x}_4)$ is a 2-composition- $\{3, 4\}$ -variate descriptor. They are descriptors

that arise from applying operators iteratively three times on the primary features: $\mathbf{X}_3 = \mathcal{O} \circ \mathcal{O} \circ \mathcal{O}(\mathbf{X}_0)$. Recall that $\mathbf{X}_1 = \mathcal{O}(\mathbf{X}_0)$ and $\mathbf{X}_2 = \mathcal{O}(\mathbf{X}_1)$. The composition of operators resembles a tree-like structure for generating descriptors and Figure 1 describes the tree-like workflow for generating the descriptor $\{\exp(\mathbf{x}_1) - \exp(\mathbf{x}_2)\}^2$.

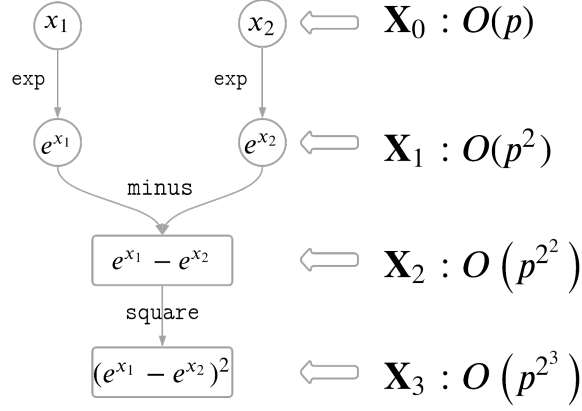


Figure 1: A tree diagram for generating $\{\exp(\mathbf{x}_1) - \exp(\mathbf{x}_2)\}^2$. The dimension of descriptor space increases double exponentially with the composition order (indicated in the figure).

To see how the dimension increases with number of iterations, let c_u and c_b denote the number of unary and binary operators, respectively, and let p_j denote the dimension of the j th descriptor space \mathbf{X}_j . Note that the dimension of \mathbf{X}_1 is $p_1 = c_u p + c_b p(p-1)/2$, which is on the order of $O(p^2)$; the dimension of \mathbf{X}_2 is $p_2 = c_u p_1 + c_b p_1(p_1-1)/2 \approx O(p^{2 \cdot 2}) = O(p^4)$; the dimension of \mathbf{X}_3 is $p_3 = c_u p_2 + c_b p_2(p_2-1)/2 \approx O(p^{2 \cdot 2 \cdot 2}) = O(p^8)$. The dimension of descriptor space will increase double exponentially with the number of binary operator compositions, e.g., with M compositions of binary operators on \mathbf{X}_0 the resulting descriptor space has a dimension of order $O(p^{2^M})$. Similarly, the double exponential expansion applies to the number of binary operators c_b . Excluding redundant descriptors does not prevent this double exponential expansion. As we show in Section 3.4, two compositions of operators in (1) on $p = 59$ primary features would yield an overwhelming descriptor space \mathbf{X}_2 containing over 5.5×10^7 descriptors even after removing redundant and non-physical descriptors. In addition, the number of active predictors will decrease with M , e.g., there are four active predictors $\exp(\mathbf{x}_1), \exp(\mathbf{x}_2), \mathbf{x}_3, \mathbf{x}_4$ in \mathbf{X}_1 , but only two active descriptors $\exp(\mathbf{x}_1) - \exp(\mathbf{x}_2)$

and $\mathbf{x}_3\mathbf{x}_4$ in \mathbf{X}_2 , and two active descriptors $\{\exp(\mathbf{x}_1) - \exp(\mathbf{x}_2)\}^2$ and $\sin(\pi\mathbf{x}_3\mathbf{x}_4)$ in \mathbf{X}_3 .

2.2 PAN descriptor selection for OIS model

We propose an iterative descriptor construction and selection procedure PAN for the OIS model, which generates descriptors by iteratively applying operators and selecting the potentially useful descriptors, i.e., the m -composition- \mathcal{S} -variate descriptors, between each iteration of descriptors synthesis. Iterative descriptor selection procedure excludes irrelevant features from descriptor generating step, achieving a *progressive* variable selection and enabling variable selection based on *ab initio* primary variables. This reduces the dimension of the subsequent descriptor space \mathbf{X}_m and mitigates collinearity among the descriptors in comparison to one-shot descriptor construction approaches.

To describe the method in its most general form, we allow different sets of operators $\mathcal{O}_m \subseteq \mathcal{O}$ for each iteration $m = 1, \dots, M$, leading to the descriptor space

$$\mathcal{O}_A^{(M)}(\mathbf{X}_0) = \mathcal{O}_M \circ \mathcal{O}_{M-1} \circ \dots \circ \mathcal{O}_2 \circ \mathcal{O}_1(\mathbf{X}_0). \quad (6)$$

We further partition the operator set \mathcal{O} into the unary operators $\mathcal{O}_u = \{I, \exp, \log, |\cdot|, \sqrt{\cdot}, ^{-1}, ^2, \sin(\pi\cdot), \cos(\pi\cdot)\}$ and the binary operators $\mathcal{O}_b = \{I, +, -, \times, /, | - |\}$. In descriptor selection, the unary operators \mathcal{O}_u induce strong collinearity among the feature engineered descriptors. For instance, in simulation we noticed that the correlation between the descriptors \mathbf{x}_1^2 and $|\mathbf{x}_1|$ exceeds 0.9 when $\mathbf{x}_1 \sim \mathcal{N}_n(\mathbf{0}, \mathbf{I})$ with $n = 200$. In addition to high correlation, the descriptor space in the OIS model exhibits another key characteristic due to binary operators \mathcal{O}_b that hampers direct applications of a variable selection method on the engineered features $(\mathbf{x}_1, \dots, \mathbf{x}_{p^*})$: an ultra-high dimension space that contains complex nonlinear descriptors. These two issues are compounded when the two operator sets are used together. Therefore, we propose to decouple the two operator sets and alternate them,

leading to two special cases of (6):

$$\mathcal{O}_{A_u}^{(M)}(\mathbf{X}_0) = \underbrace{\cdots \mathcal{O}_b \circ \mathcal{O}_u \circ \mathcal{O}_b \circ \mathcal{O}_u}_{M \text{ times}}(\mathbf{X}_0) \quad (7)$$

$$\mathcal{O}_{A_b}^{(M)}(\mathbf{X}_0) = \underbrace{\cdots \mathcal{O}_u \circ \mathcal{O}_b \circ \mathcal{O}_u \circ \mathcal{O}_b}_{M \text{ times}}(\mathbf{X}_0) = \mathcal{O}_{A_u}^{(M-1)} \circ \mathcal{O}_b(\mathbf{X}_0). \quad (8)$$

Note the descriptor spaces $\mathcal{O}_{A_u}^{(M)}(\mathbf{X}_0)$ and $\mathcal{O}_{A_b}^{(M)}(\mathbf{X}_0)$ are not equivalent to the full descriptor space $\mathcal{O}^{(M)}(\mathbf{X}_0)$ with the same order of compositions M . However, it is easy to see that $\mathcal{O}_{A_u}^{(M_u)}(\mathbf{X}_0)$ and $\mathcal{O}_{A_b}^{(M_b)}(\mathbf{X}_0)$ can recover the full descriptor space $\mathcal{O}^{(M)}(\mathbf{X}_0)$ with some $M_u > M$ and $M_b > M$, respectively. For instance, consider the 2-composition descriptor space $\mathcal{O}^{(2)}(\mathbf{X}_0)$ generated using (3). It contains descriptors such as $f_1 = (x_i^2 + x_j^2)$ and $f_2 = (x_i + x_j)^2$. These two descriptors can be generated using $\mathcal{O}_{A_b}^{(M)}(\mathbf{X}_0)$ in (8) as follows: $f_1 = \text{add} \circ \text{square} \circ I(x_i, x_j) \in \mathcal{O}_{A_b}^{(3)}(\mathbf{X}_0)$ and $f_2 = \text{square} \circ \text{add}(x_i, x_j) \in \mathcal{O}_{A_b}^{(2)}(\mathbf{X}_0)$. Similarly, we can use (7) to generate the two descriptors as follows: $f_1 = \text{add}(\text{square}(x_i), \text{square}(x_j)) \in \mathcal{O}_{A_u}^{(2)}(\mathbf{X}_0)$ and $f_2 = \text{square} \circ \text{add}(I(x_i), I(x_j)) \in \mathcal{O}_{A_u}^{(3)}(\mathbf{X}_0)$. As such, under the M -composition- \mathcal{S} -variate OIS model in (4), one may consider to use $\mathcal{O}^{(M)}$, $\mathcal{O}_{A_u}^{(M)}(\mathbf{X}_0)$, or $\mathcal{O}_{A_b}^{(M)}(\mathbf{X}_0)$ as long as the true descriptors are contained in the generated descriptor space. In what follows we will focus on $\mathcal{O}_{A_u}^{(M)}(\mathbf{X}_0)$ and $\mathcal{O}_{A_b}^{(M)}(\mathbf{X}_0)$ instead of $\mathcal{O}^{(M)}$ for their aforementioned advantages, without loss of generality.

The framework of our iterative descriptor selection procedure is as follows.

PAN descriptor selection procedure:

1. **Repeat** the following until descriptors exhibit a strong linear association with the response variable \mathbf{y} ($i = 0$):
 - (a) Use a nonparametric variable selection procedure to perform descriptor selection on \mathbf{X}_i and obtain the selected descriptors \mathbf{X}'_i
 - (b) Apply the i th operator set \mathcal{O}_i on all of the previously selected descriptors, $\bigcup_m \mathbf{X}'_m$, yielding a new descriptor space, $\mathbf{X}_{i+1} = \mathcal{O}_i(\bigcup_m \mathbf{X}'_m)$
 - (c) Increase counter: $i = i + 1$

2. **Once** there exist descriptor(s) that exhibit a strong linear association with response variable \mathbf{y} , use a linear parametric variable selection procedure to perform descriptor selection on \mathbf{X}_i , and obtain the selected descriptors, $\mathbf{X}^* \subseteq \mathbf{X}_i$.

To see how this iterative procedure may reduce the dimension of descriptor space significantly, let $s_i = |\mathbf{X}'_i|$ be the number of descriptors selected in the i th iteration and $p_i = |\mathbf{X}_i|$ be the number of descriptors in the i th descriptor space. Suppose that the number of selected descriptors is sparse in each iteration, i.e., $s_i \ll p_i$. Then the size of the next descriptor space $p_{i+1} = |\mathbf{X}_{i+1}|$ is on the order of $O(s_i^2) \ll O(p_i^2)$, assuming binary operators were used, and this holds for all iteration $i \geq 0$. If we further assume $s_i \approx O(p)$ for all $i \geq 0$, where $p = |\mathbf{X}_0|$ is the number of primary features, then the size of the $(i + 1)$ th descriptor space \mathbf{X}_{i+1} is on the order of $O(p^2)$, compared to $O(p^{2^{i+1}})$ for the one-shot descriptor selection procedures. Note these assumptions are reasonable according to the discussion in Section 2.1. In the simulation study in Section 3.4 with $p = 10$ primary features, we observed that $s_i \approx O(10^1)$ and $p_i \approx O(10^2)$ for all iterations of PAN procedure. On the contrary, a one-shot descriptor selection procedure, SISSO, generates a descriptor space containing 9.26×10^9 descriptors in the same setting. Thus, in this example the proposed iterative descriptor selection approach PAN generates a final descriptor space with $O(p^2)$ descriptors, dramatically reducing the dimension.

We employ a nonparametric variable selection procedure in Step 1(a) because the low composition complexity descriptors do not necessarily exhibit a strong linear association with the response variable. Thus, a nonparametric variable selection method that accounts for flexible modeling of the effect of intermediate descriptors is more suitable for preliminary screening of the fundamental structure of the descriptors. In Step 2, a linear parametric variable selection method is adopted to gain statistical power as a strong linear association between the response and descriptors emerges.

However, not all nonparametric variable selection procedures are suitable in Step 1(a). Compositions of operators on the primary features inevitably generate strong collinearity among predictors. Since nonparametric models can learn nonlinear structures between

predictors and response, predictors that are constructed from the same set of primary features but differ in the composition of operators are potentially no different to a nonparametric variable selection method. For instance, suppose the true model is $\mathbf{y} = f_1(\mathbf{x}_1) + \varepsilon$ and both $f_1(\mathbf{x}_1)$ and $f_2(\mathbf{x}_1)$ are descriptors for the response \mathbf{y} . A nonparametric variable selection method may select $f_1(\mathbf{x}_1)$ and $f_2(\mathbf{x}_1)$ with equal chance but we want $f_1(\mathbf{x}_1)$ to be selected with high probability. Thus, it is crucial for a nonparametric variable selection method to enjoy an OIS screening property (defined in Section 2.3) when strong collinearity or ambiguity is present. In this article, we employ a Bayesian additive regression trees-based variable selection procedure (Bleich et al., 2014) in Step 1(a), and we demonstrate that it interestingly enjoys the OIS screening property in finite sample assessment in Section 3.

BART is a Bayesian nonparametric ensemble tree method for modeling $\mathbf{y} = f(\mathbf{X}) + \varepsilon$, the unknown relationship between a response vector \mathbf{y} and a set of predictors $\mathbf{x}_1, \dots, \mathbf{x}_p$ (Chipman et al., 2010). More specifically, BART models the regression function f by a sum of regression trees

$$\mathbf{y} = \sum_{i=1}^m g_i(\mathbf{x}_1, \dots, \mathbf{x}_p; \mathcal{T}_i, \boldsymbol{\mu}_i) + \varepsilon, \quad \varepsilon \sim \mathcal{N}_n(\mathbf{0}, \sigma^2 \mathbf{I}_n).$$

Each binary regression tree g_i consists of two parts: a tree structure \mathcal{T}_i which partitions observations into a set of B_i terminal nodes and a set of terminal parameters $\boldsymbol{\mu}_i = \{\mu_{i1}, \dots, \mu_{iB_i}\}$ that are attached to the terminal nodes such that each predictor contained in the same terminal node b shares the same terminal value μ_{ib} .

The prior distributions for $(\mathcal{T}_i, \boldsymbol{\mu}_i)$ constrain each tree to be small and thereby avoid overlapping in trees. In essence, BART is an ensemble of weak learners, each contributing to approximate the unknown function in a small and distinct fashion. The prior for the variance σ^2 is an inverse chi-square distribution $\nu\lambda/\chi_\nu^2$ with hyperparameters (ν, λ) . Readers are referred to Chipman et al. (2010) for the full details of BART and posterior sampling.

The primary usage of BART is prediction, and the predicted values $\hat{\mathbf{y}}$ for the response variable \mathbf{y} serve no purpose in variable selection. However, a variable inclusion rule can be

defined based on the variable inclusion proportion q_i , which can be easily estimated from the posterior samples. The main challenge in defining such a rule is to determine a selection threshold of the variable inclusion proportion for \mathbf{x}_i to be selected. To this end, we adopt the permutation-based selection threshold based on the permutation null distribution of $\mathbf{q} = (q_1, \dots, q_p)$ proposed by Bleich et al. (2014).

Specifically, B permutations of the response vector $\mathbf{y}_1^*, \dots, \mathbf{y}_B^*$ are generated, and a BART model is fitted for each of the permuted response vector with the same predictors $\mathbf{x}_1, \dots, \mathbf{x}_p$. The variable inclusion proportions $\mathbf{q}_1^*, \dots, \mathbf{q}_B^*$ from the permuted BART model are then used to create a permutation null distribution for the variable inclusion proportion \mathbf{q} . Then the predictor \mathbf{x}_i is selected if $q_i > m_i + C^* \cdot s_i$, where m_i and s_i are the mean and standard deviation of variable inclusion proportion q_i^* across all permutations, and $C^* = \inf_{C \in \mathbb{R}^+} \left\{ \forall i, \frac{1}{B} \sum_{b=1}^B \mathbb{I}(q_{i,b}^* \leq m_i + C \cdot s_i) > 1 - \alpha \right\}$ is the smallest global standard error multiplier (G.SE) that gives a simultaneous $1 - \alpha$ coverage across the permutation null distributions of q_i for all predictor variables; here $q_{i,b}^*$ is the i th element of \mathbf{q}_b^* for $1 \leq i \leq n$ and $1 \leq b \leq B$. We herein refer to this BART-based variable selection procedure as BART-G.SE, and the PAN descriptor selection procedure with BART-G.SE as the nonparametric variable selection module as iBART.

2.3 OIS screening property

We introduce the notion of OIS screening property, a crucial characterization of the desired nonparametric modules in PAN that also distinguishes descriptor selection from traditional variable selection. Suppose the true data generating model is

$$\mathbf{y} = f(\mathbf{X}) + \boldsymbol{\varepsilon} = f(\mathbf{X}_{\mathcal{S}_0}) + \boldsymbol{\varepsilon}, \quad (9)$$

where $\mathbf{X} = (\mathbf{x}_1, \dots, \mathbf{x}_p)$ collects p primary features and $\mathcal{S}_0 \subseteq [p]$ is the set of active indices. A frequently used property to assess nonparametric variable selection methods is variable selection consistency, which is defined as the successful selection of the active index set

\mathcal{S}_0 asymptotically. In the OIS framework, however, the goal is not only to identify the active primary features $\mathbf{X}_{\mathcal{S}_0}$ but also to identify the compositions of operators that recover the underlying function f . This calls for a new property for selection accuracy in the OIS framework. To illustrate such a need, let us consider the following example. Suppose the underlying function $f(\cdot)$ in (9) is $f(\mathbf{x}_1) = \mathbf{x}_1^2$ and suppose the engineered features $\{\mathbf{x}_1, \dots, \mathbf{x}_{p^*}\}$ in the OIS model are $\mathcal{O}_u(\mathbf{X})$, i.e., unary transformations of the primary features $\mathbf{x}_1, \dots, \mathbf{x}_p$ such as $\mathbf{x}_i, \mathbf{x}_i^2, \sqrt{\mathbf{x}_i}, i = 1, \dots, p$. Traditional nonparametric variable selection may not make a distinction between \mathbf{x}_1 and $f(\mathbf{x}_1) = \mathbf{x}_1^2$, but here we consider selecting the active descriptor $f(\mathbf{x}_1) = \mathbf{x}_1^2$ as descriptor selection not only selects active primary variables but also active operators. This discrepancy is amplified by the iterative structure in OIS, and that the OIS model is assumed to be linear while the nonparametric method only serves as a dimension reduction tool.

With the M -composition- \mathcal{S} -variate OIS model in (4), we now introduce the OIS screening property. We assume that the true model follows an M_0 -composition- \mathcal{S}_0 -variate OIS model, where M_0 and \mathcal{S}_0 denote the true composition complexity and active index set, respectively.

Definition 2.3 (OIS screening property). *Suppose that the descriptor space is the class of M_0 -composition descriptors $\mathbf{X}_{M_0} = \mathcal{O}^{(M_0)}(\mathbf{X})$. A variable selection procedure enjoys the OIS screening property if the M_0 -composition- \mathcal{S}_0 -variate descriptors $f_1^{(M_0, \mathcal{S}_0)}(\mathbf{X}_{\mathcal{S}_0}), \dots, f_K^{(M_0, \mathcal{S}_0)}(\mathbf{X}_{\mathcal{S}_0})$ survive the variable selection process.*

Note that if a descriptor selection procedure only constructs up to m -composition descriptors $\mathbf{X}_m = \mathcal{O}^{(m)}(\mathbf{X})$, where m is less than the true composition complexity M_0 , then it will not enjoy the OIS screening property. For descriptors selection procedures that require a user-defined composition complexity, such as SISSO, it is thus possible that the procedure will not enjoy OIS screening property simply due to an incorrect user-specified composition complexity. The following notation extends the OIS screening property to describe the successful recovery of lower composition complexity descriptors.

Definition 2.4 ((m_0, \mathcal{S}_0) -OIS screening property). *Suppose that the descriptor space is the class of m -composition descriptors $\mathbf{X}_m = \mathcal{O}^{(m)}(\mathbf{X})$, where $0 \leq m \leq M_0$. We say that a variable selection procedure satisfies the (m_0, \mathcal{S}_0) -OIS screening property, or is simply (m_0, \mathcal{S}_0) -OIS for short, if the m_0 -composition- \mathcal{S}_0 -variate descriptors $f_1^{(m_0, \mathcal{S}_0)}(\mathbf{X}_{\mathcal{S}_0}), \dots, f_K^{(m_0, \mathcal{S}_0)}(\mathbf{X}_{\mathcal{S}_0})$ survive the variable selection process, where $0 \leq m_0 \leq m$ and m_0 is the highest nontrivial composition complexity among the K descriptors.*

We demonstrate the OIS screening property using the example in (5). Recall that the first descriptor $\{\exp(\mathbf{x}_1) - \exp(\mathbf{x}_2)\}^2$ in (5) is a 3-composition- $\{1, 2\}$ -variate descriptor. A descriptor selection procedure is $(0, \mathcal{S}_0)$ -OIS if it selects \mathbf{x}_1 and \mathbf{x}_2 , $(1, \mathcal{S}_0)$ -OIS if selects $\exp(\mathbf{x}_1)$ and $\exp(\mathbf{x}_2)$, $(2, \mathcal{S}_0)$ -OIS if selects $\exp(\mathbf{x}_1) - \exp(\mathbf{x}_2)$, and $(3, \mathcal{S}_0)$ -OIS if selects $\{\exp(\mathbf{x}_1) - \exp(\mathbf{x}_2)\}^2$. Here a $(3, \mathcal{S}_0)$ -OIS descriptor selection procedure possesses the OIS screening property.

For an iterative descriptor selection procedure such as the proposed PAN method, a sufficient condition for the OIS screening property is that it is $(1, \mathcal{S}_0)$ -OIS in all iterations, provided that the procedure iterates until true composition complexity M_0 is reached. We state and prove this simple but useful result in the following proposition.

Proposition 2.1. *Suppose the true model follows an M_0 -composition- \mathcal{S}_0 -variate OIS model and an iterative descriptor selection procedure iterates $M' \geq M_0$ times until the class of M_0 -composition descriptors $\mathcal{O}^{(M_0)}(\mathbf{X})$ is generated. Then the iterative procedure satisfies the OIS screening property if it satisfies $(1, \mathcal{S}_0)$ -OIS screening property in the m th iteration with \mathbf{X}_m treated as the primary features, for all $0 \leq m \leq M'$.*

Proof. Let k_m denote the number of active m -composition- \mathcal{S}_0 -variate descriptors in iteration m , where $0 \leq m \leq M'$. Based on the assumption of Proposition 2.1, we know that the lower composition complexity descriptors $f_1^{m, \mathcal{S}_0}(\mathbf{X}), \dots, f_{k_m}^{m, \mathcal{S}_0}(\mathbf{X})$ are selected by the iterative descriptor selection procedure in all iterations $0 \leq m \leq M'$. Thus, the true descriptors $f_1^{M_0, \mathcal{S}_0}(\mathbf{X}), \dots, f_K^{M_0, \mathcal{S}_0}(\mathbf{X})$ are selected by the iterative procedure, which implies that the iterative procedure satisfies OIS screening property. \square

Proposition 2.1 indicates that iBART satisfies the OIS screening property if BART-G.SE is $(1, \mathcal{S}_0)$ -OIS in each iteration. Since either unary or binary operators are applied in each iteration, we examine in Section 3 whether the $(1, \mathcal{S}_0)$ -OIS screening property holds for BART-G.SE when either unary or binary operators are applied to primary features. In general, one can replace BART-G.SE with any $(1, \mathcal{S}_0)$ -OIS variable selection procedure in our iterative framework, and the resulting procedure will enjoy the full OIS screening property. In Section 3.4, we compare various descriptor selection procedures under a 3-composition OIS model and show that iBART enjoys OIS screening property.

2.4 Practical consideration and the algorithm

We adopt the descriptor generating strategies in (7) and (8) for different scenarios. We recommend the descriptor generating process in (8) when there is strong collinearity among the primary features \mathbf{X}_0 . This is because the unary operators \mathcal{O}_u aggravate collinearity among descriptors and thus increase the number of false positives (FP) in the first iteration of iBART. These FPs will accumulate as iteration goes on, leading to worse performance. On the other hand, we suggest the descriptor generating process in (7) when there is no strong collinearity among the primary features \mathbf{X}_0 .

The stopping criterion in Step 1 can be easily modified depending on the practical need. For example, we can specify the maximum composition complexity M_{\max} in the algorithm, like SISSO, or we can have a data-driven stopping criterion that terminates Step 1 when there exists a descriptor such that its absolute correlation with response variable \mathbf{y} exceeds a pre-specified threshold, $\rho_{\max} \in (0, 1)$. We note that iBART allows much larger M_{\max} than SISSO as iBART does not rely on one-short feature engineering.

It is also common in practice that one may only want to select k descriptors for easy interpretation, such as $k \leq 5$. If the cardinality of the selected descriptors \mathbf{X}^* is greater than k , then an ℓ_0 -penalized regression may be used to choose the best k descriptors.

We allow user-specified options for these considerations when implementing the proposed method iBART, summarized in Algorithm 1. The default settings are specified as follows,

which will be used in our experiments. We use the BART-G.SE thresholding variable selection procedure implemented in the R package `bartMachine` to perform nonparametric variable selection for Step 1(a) in PAN and use LASSO implemented in the R package `glmnet` to perform parametric variable selection for Step 2 in PAN. For BART-G.SE, we set the number of trees to 20, the number of burn-in samples to 10,000, the number of posterior samples to 5,000, the number of permutations of the response to 50, and the rest of the parameters to the default values. We choose the penalty term λ in LASSO via 10-fold cross validation and set the other parameters to the default values. The algorithm terminates if the composition complexity M reaches $M_{\max} = 4$ or the maximum absolute correlation $|\rho|$ reaches $\rho_{\max} = 0.95$, whichever occurs first.

Algorithm 1: iBART

Input: $\rho_{\max} \in (0, 1)$ = maximum absolute correlation with the response variable;
 M_{\max} = maximum composition complexity;
 $Lzero$ = whether to perform ℓ_0 -penalized regression;
 k = number of selected descriptors by ℓ_0 -penalized regression. Only required when $Lzero == \text{TRUE}$.
Output: \mathbf{X}_k^* : selected descriptors
Data: \mathbf{X}_0 : primary features; \mathcal{O}_u : set of unary operators; \mathcal{O}_b : set of binary operators; \mathbf{y} : response vector

```

1  $M = 0$ 
2  $\rho = \max_{\mathbf{x} \in \mathbf{X}_M} \text{cor}(\mathbf{x}, \mathbf{y})$ 
3 while  $M \leq M_{\max}$  or  $|\rho| \leq \rho_{\max}$  do
4    $\mathbf{X}'_M \leftarrow$  BART-G.SE selected descriptors on  $\mathbf{X}_M$ 
5    $\mathbf{X}_{M+1} \leftarrow \mathcal{O}_{M+1} (\cup_i \mathbf{X}'_i)$ 
6    $M \leftarrow M + 1$ 
7    $\rho \leftarrow \max_{\mathbf{x} \in \mathbf{X}_M} \text{cor}(\mathbf{x}, \mathbf{y})$ 
8 end
9  $\mathbf{X}^* \leftarrow$  LASSO selected descriptors on  $\mathbf{X}_M$ 
10 if  $Lzero == \text{TRUE}$  and  $|\mathbf{X}^*| > k$  then
11    $\mathbf{X}_k^* \leftarrow$  best  $k$  descriptors from  $\ell_0$ -penalized regression
12 end
13 else
14    $\mathbf{X}_k^* \leftarrow \mathbf{X}^*$ 
15 end
```

3 Simulation

3.1 Outline

In Sections 3.2 and 3.3 we demonstrate using simulations that BART-G.SE is $(1, \mathcal{S}_0)$ -OIS when the predictors are either unary or binary transformations of primary features. This interesting property hints that iBART enjoys the OIS screening property in view of Proposition 2.1. In Section 3.4 we compare iBART to several methods and show iBART indeed achieves the OIS screening property using a more complex and realistic simulation setting. Section 3.5 showcases the robustness of iBART in the initial input dimension p . We use Algorithm 1 and the default settings described in Section 2.4 when implementing the proposed method, unless stated otherwise. Each simulation is replicated 50 times.

3.2 Unary operators

We consider all unary transformations of five primary features $\mathbf{X} = (\mathbf{x}_1, \dots, \mathbf{x}_5)$, i.e., the descriptor space is $\mathcal{O}_u(\mathbf{X}) = \bigcup_{i=1}^5 \{\mathbf{x}_i, \mathbf{x}_i^{-1}, \mathbf{x}_i^2, \sqrt{\mathbf{x}_i}, \log(\mathbf{x}_i), \exp(\mathbf{x}_i), |\mathbf{x}_i|, \sin(\pi \mathbf{x}_i), \cos(\pi \mathbf{x}_i)\}$. For each unary operator $u_i \in \mathcal{O}_u$, we generate the response vector by

$$\mathbf{y} = 10u_i(\mathbf{x}_1) + \boldsymbol{\varepsilon}, \quad \boldsymbol{\varepsilon} \sim \mathcal{N}_n(\mathbf{0}, \mathbf{I}) \quad (10)$$

with sample size $n = 200$, yielding eight independent models in total. We draw the primary features $\mathbf{x}_1, \dots, \mathbf{x}_5$ from a normal or lognormal distribution as follows:

$$\begin{cases} \mathbf{x}_1, \dots, \mathbf{x}_5 \stackrel{\text{i.i.d.}}{\sim} \mathcal{N}_n(\mathbf{0}, \mathbf{I}), & \text{if } u_i : \mathbb{R} \rightarrow \mathbb{R}, \\ \mathbf{x}_1, \dots, \mathbf{x}_5 \stackrel{\text{i.i.d.}}{\sim} \text{Lognormal}(2, 0.5), & \text{if } u_i : \mathbb{R}_{\geq 0} \rightarrow \mathbb{R}_{\geq 0}. \end{cases}$$

The left plot in Figure 2a shows the number of true positive (TP) of BART-G.SE for each of the eight models in (10). The number of TP is one 50/50 times for all eight models. This suggests that BART-G.SE is capable of identifying the true descriptor with high

probability when the descriptor space is populated with unary operators \mathcal{O}_u . Thus, it enjoys $(1, \mathcal{S}_0)$ -OIS screening property under the simulation models (10).

The left plot in Figure 2b shows the number of false positive (FP) of BART-G.SE for each simulation setting. Although BART-G.SE is capable of capturing the active descriptor with high probability, it also selects some inactive descriptors in some cases. The number of FP is especially high when the active descriptor is $|\mathbf{x}_1|$, $\exp(\mathbf{x}_1)$, $\log(\mathbf{x}_1)$, \mathbf{x}_1^2 , or $\sqrt{\mathbf{x}_1}$. This is due to high collinearity among these four descriptors. In particular, the empirical Pearson correlation between $\log(\mathbf{x}_1)$ and $\sqrt{\mathbf{x}_1}$ is over 0.99 under simulation setting (10), and thus some false positives are expected. Selecting inactive descriptors in one iteration is less a concern in variable selection with OIS as they do not constitute misspecified models, and can be further screened out using Step 2 of PAN.

3.3 Binary operators

We examine whether $(1, \mathcal{S}_0)$ -OIS screening property holds for BART-G.SE when binary operators $\mathcal{O}_b = \{+, -, \times, /, | - |\}$ are used with five primary features $\mathbf{X}_0 = (\mathbf{x}_1, \dots, \mathbf{x}_5)$. That is, the descriptor space $\mathcal{O}_b(\mathbf{X}_0) \in \mathbb{R}^{200 \times 55}$ contains all binary transformations of all possible pairs of the five primary features. For each binary operator $b_i \in \mathcal{O}_b$, we generate the response vector by

$$\mathbf{y} = 10b_i(\mathbf{x}_1, \mathbf{x}_2) + \boldsymbol{\varepsilon}, \quad \boldsymbol{\varepsilon} \sim \mathcal{N}_n(\mathbf{0}, \mathbf{I}) \quad (11)$$

with sample size $n = 200$, yielding a total of five independent models. We generate the primary features \mathbf{X}_0 following $\mathbf{x}_1, \dots, \mathbf{x}_5 \stackrel{\text{i.i.d.}}{\sim} \mathcal{N}_n(\mathbf{0}, \mathbf{I})$.

The right plot in Figure 2a shows the number of TP for each of the five models in (11). BART-G.SE is able to identify the true binary descriptor 50/50 times in all five settings, similar to earlier observations in Section 3.2. Thus, BART-G.SE enjoys $(1, \mathcal{S}_0)$ -OIS screening property under this simulation setting.

The right plot in Figure 2b shows that BART-G.SE may also select some irrelevant

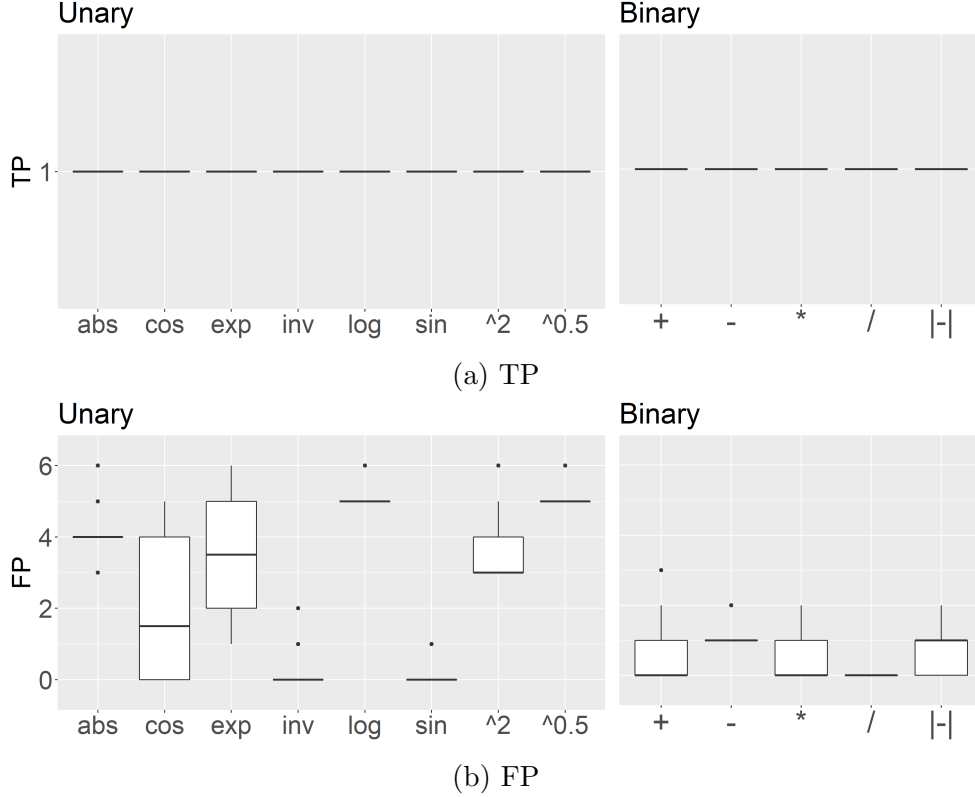


Figure 2: Boxplots of TP and FP over 50 simulations under models (10) and (11).

descriptors but considerably fewer than observed in Section 3.2. In particular, when the true descriptor is $(\mathbf{x}_1 - \mathbf{x}_2)$, BART-G.SE correctly selects $(\mathbf{x}_1 - \mathbf{x}_2)$ but also falsely selects $|\mathbf{x}_1 - \mathbf{x}_2|$ 50/50 times. Unlike previous findings in Section 3.2, the reason for such behavior is not due to high correlation between $|\mathbf{x}_1 - \mathbf{x}_2|$ and $(\mathbf{x}_1 - \mathbf{x}_2)$. In fact, their empirical Pearson correlation is merely 0.07. We suspect that $|\mathbf{x}_1 - \mathbf{x}_2|$ was selected due to its trivial nonlinear association with $(\mathbf{x}_1 - \mathbf{x}_2)$. Similarly, BART-G.SE selects both $(\mathbf{x}_1 - \mathbf{x}_2)$ and $|\mathbf{x}_1 - \mathbf{x}_2|$ with high probability when the true descriptor is $|\mathbf{x}_1 - \mathbf{x}_2|$. On the other hand, when the true descriptor is $(\mathbf{x}_1 + \mathbf{x}_2)$, $\mathbf{x}_1 \times \mathbf{x}_2$, or $\mathbf{x}_1/\mathbf{x}_2$, the FP rate of BART-G.SE is nearly identical to zero. We observe that the FP rate of BART-G.SE is systematically lower when the descriptor space is populated with binary transformations than with unary transformations. This aligns with our expectation since binary transformations do not induce high collinearity while unary transformations do.

Sections 3.2 and 3.3 show that BART-G.SE enjoys $(1, \mathcal{S}_0)$ -OIS screening property under the respective simulation settings, strongly suggesting the full OIS screening property of

iBART according to Proposition 2.1. In Section 3.4, we carry out a more complex simulation in which we observe that iBART indeed continues to enjoy the OIS screening property.

3.4 Complex descriptors with high-order compositions

In this section, we compare iBART with existing approaches under a complex and realistic model and demonstrate superior performance of iBART. We use the following model

$$\mathbf{y} = 15\{\exp(\mathbf{x}_1) - \exp(\mathbf{x}_2)\}^2 + 20\sin(\pi\mathbf{x}_3\mathbf{x}_4) + \boldsymbol{\varepsilon}, \quad \boldsymbol{\varepsilon} \sim \mathcal{N}_n(\mathbf{0}, \sigma^2 \mathbf{I}), \quad (12)$$

with $n = 250$, $p = 10$, and $\sigma = 0.5$. Here the number of primary features p is set to a relatively small number since competing one-shot methods cannot complete the simulation when $p \geq 20$ due to the ultra-high dimension of the descriptor space. In Section 3.5, we demonstrate that iBART scales well in p and gives robust performance. The operator space is $\mathcal{O} = \{+, -, \times, /, | - |, I, ^{-1}, ^2, \sqrt{\cdot}, \log, \exp, |\cdot|, \sin(\pi\cdot), \cos(\pi\cdot)\}$, and the primary feature vectors \mathbf{x}_i are drawn from a uniform distribution, namely, $\mathbf{x}_1, \dots, \mathbf{x}_p \stackrel{\text{i.i.d.}}{\sim} \text{U}_n(-1, 1)$.

iBART is implemented in R based on Algorithm 1 in Section 2.4 using the default settings. We chose the descriptor generating process (7) in Section 3 since the i.i.d. primary features do not show strong collinearity. Two versions of iBART are considered: iBART with and without ℓ_0 -penalized regression, labeled as “iBART” and “iBART+ ℓ_0 ”, respectively. The ℓ_0 -penalization selects the best subset of k variables by the Akaike information criterion (AIC) with $k \in \{1, 2, 3, 4\}$. We compare the performance of iBART and iBART+ ℓ_0 with SISSO and LASSO. SISSO is implemented using the Fortran 90 program published by Ouyang et al. (2018) on GitHub with the following settings: the absolute upper and lower bounds of descriptors are set to 1×10^5 and 1×10^{-6} , respectively; the size of the SIS-selected subspace is set to 20; the operator composition complexity is set to 3; the maximum number of operators in a descriptor is set to 6; and the number of selected descriptors $k \in \{1, 2, 3, 4\}$ is tuned by AIC. The R package `glmnet` is used to implement LASSO and the penalty parameter λ is tuned via 10-fold cross validation. Since the size of $\mathcal{O}^{(3)}(\mathbf{X}_0)$ exceeds the

limit of an \mathbf{R} matrix, we give LASSO an advantage by reducing the descriptor space to $\mathcal{O}_u \circ \mathcal{O} \circ \mathcal{O}(\mathbf{X}_0)$ that aligns with the true data generating process. We also utilize the ℓ_0 -penalized regression step as in SISSO and iBART+ ℓ_0 for LASSO, leading to LASSO+ ℓ_0 .

For each method, we calculate the number of true positive (TP) selections, false positive (FP) selections, and false negative (FN) selections. We use the F_1 score as an overall metric to quantify the performance of each method: $F_1 = 2 \cdot \frac{\text{Precision} \cdot \text{Recall}}{\text{Precision} + \text{Recall}}$, where $\text{Precision} = \frac{\text{TP}}{\text{TP} + \text{FP}}$ and $\text{Recall} = \frac{\text{TP}}{\text{TP} + \text{FN}}$. The value $F_1 = 1$ means correct identification of the true model without having any FP and FN. In this simulation, the two true positives are $f_1(\mathbf{X}) = \{\exp(\mathbf{x}_1) - \exp(\mathbf{x}_2)\}^2$ and $f_2(\mathbf{X}) = \sin(\pi \mathbf{x}_3 \mathbf{x}_4)$.

Figure 3 entails the F_1 scores of all descriptor selection methods. Both iBART-based methods achieve very high F_1 scores, with a median F_1 score of 0.8 and 1 for iBART and iBART+ ℓ_0 , respectively. In particular, both iBART and iBART+ ℓ_0 have 2 TPs in all simulations while incurring 0.8 FPs and 0.22 FPs on average, respectively. This demonstrates that iBART enjoys the OIS screening property as it is able to identify the positive descriptors 50/50 times in simulations. Furthermore, iBART+ ℓ_0 gives a very low FP rate, scoring a perfect F_1 score 48/50 times. LASSO-based methods and SISSO have lower F_1 scores than iBART and iBART+ ℓ_0 but for different reasons. LASSO selects 32 descriptors on average, and the 2 TPs are always selected. This means that LASSO also enjoys the OIS screening property but its F_1 score is hindered by the large number of FP. With the help of the ℓ_0 -penalized regression, LASSO+ ℓ_0 reduces the average number of FP from 30 to 2 while maintaining two TPs 50/50 times, substantially increasing the F_1 score to around 0.70, the third-highest score but still considerably lower than iBART and iBART+ ℓ_0 . SISSO, on the other hand, has only 1 TP but 3 FPs in all simulations, which unfortunately does not satisfy the OIS screening property. In particular, SISSO can identify $\sin(\pi \mathbf{x}_3 \mathbf{x}_4)$ 50/50 times but always selects $|\exp(\mathbf{x}_1) - \exp(\mathbf{x}_2)|$, a descriptor that has absolute correlation over 0.9 with the true descriptor, $\{\exp(\mathbf{x}_1) - \exp(\mathbf{x}_2)\}^2$. In summary, both iBART-based and LASSO-based methods satisfy the OIS screening property but LASSO-based methods incur higher FPs. SISSO, however, fails to identify one of the two descriptors 50/50 times

but selects a highly correlated counterpart, indicating its relatively weakened ability to distinguish the true descriptor when there are descriptors highly correlated with the truth.

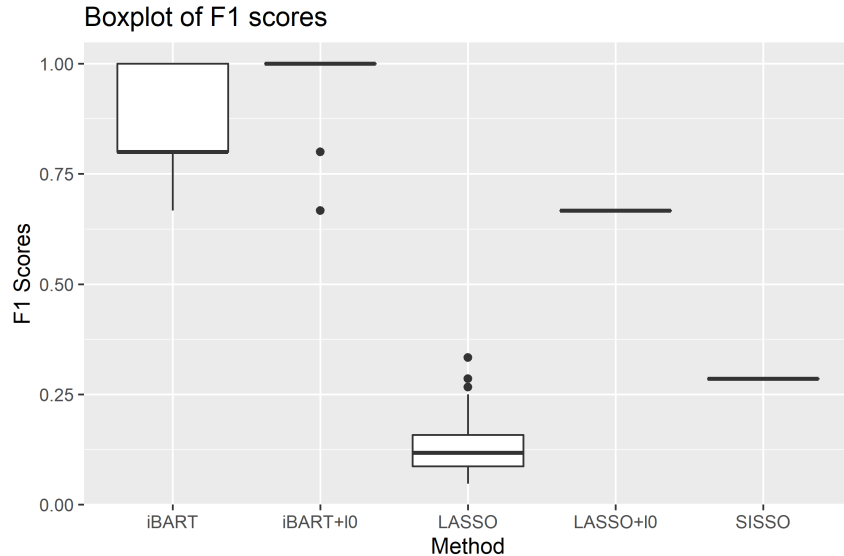


Figure 3: Boxplots of F_1 scores over 50 simulations for different methods under Model (12).

To gain insight into the scalability of iBART, Figure 4 shows the mean number of iBART generated and selected descriptors in each iteration. The mean number of iBART generated descriptors is no greater than $158 \leq 1.5p^2$ in each iteration and is significantly less than the number of descriptors generated by SISSO and LASSO, 9.26×10^9 and 1.2×10^6 , respectively. Such dimension reduction not only lessens the runtime and memory usage but also enables iBART to tackle data with much larger p , as we show in Sections 3.5 and 4.

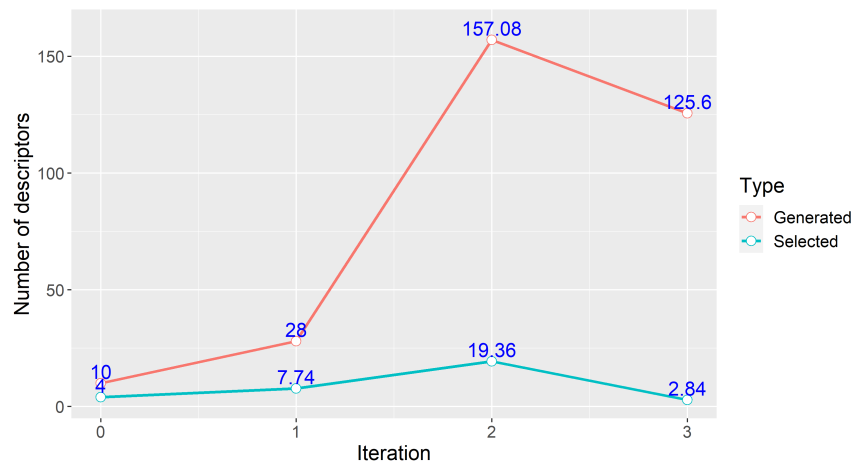


Figure 4: Mean number of iBART generated and selected descriptors in each iteration.

3.5 Large p

In this section, we demonstrate that the performance of iBART is robust to increase in input dimension p while one-shot descriptor selection methods are not. Under Model (12) with $p = 20$, SISSO with the same parameter settings in the preceding section generates more than 3.8×10^{11} descriptors, and failed to complete one simulation within 24 hours on a server with 1.3TB of memory and 40 CPU cores available to SISSO. LASSO, on the other hand, failed at $p = 20$ since the `glmnet` function in the R package `glmnet` cannot handle a matrix of size $250 \times (1.57 \times 10^7)$. The proposed method iBART instead scales well in the input dimension p partly because of the efficient dimension reduction via the PAN strategy.

We implement iBART for $p \in \{10, 20, 50, 100, 200\}$ using the same simulation settings in Section 3.4. Figure 5 shows that iBART’s F_1 score is robust to the increase in p . In fact, benefiting from the *ab initio* mechanism through the PAN strategy, the performance of iBART would be identical for varying p as long as it selects $\mathbf{x}_1, \mathbf{x}_2, \mathbf{x}_3, \mathbf{x}_4$ in the first iteration, which is often the case based on Figure 5. In contrast, one-shot descriptor selection methods suffer significantly from just a small increase in the input dimension p since the descriptor space increases double exponentially in p . One way for one-shot description selection to circumvent the ultra-high dimension phenomenon with large p is to reduce the maximum order of composition complexity. However, this undesirably rules out descriptors with the correct composition complexity. For example, the descriptor in (12) $f_1(\mathbf{x}) = \{\exp(\mathbf{x}_1) - \exp(\mathbf{x}_2)\}^2$ requires at least 3 compositions of operators, and reducing the number of compositions to 2 means that $f_1(\mathbf{x})$ would never be generated and hence would never be selected. Thus, one-shot descriptor selection methods cannot generate and select complex descriptors unless the number of primary feature p is small. We have considered a small $p = 10$ in the preceding section to accommodate such limitation of one-shot methods. A common practice when adopting one-shot methods for large p in real data applications typically resorts to ad hoc adaptation, as demonstrated in the next section.

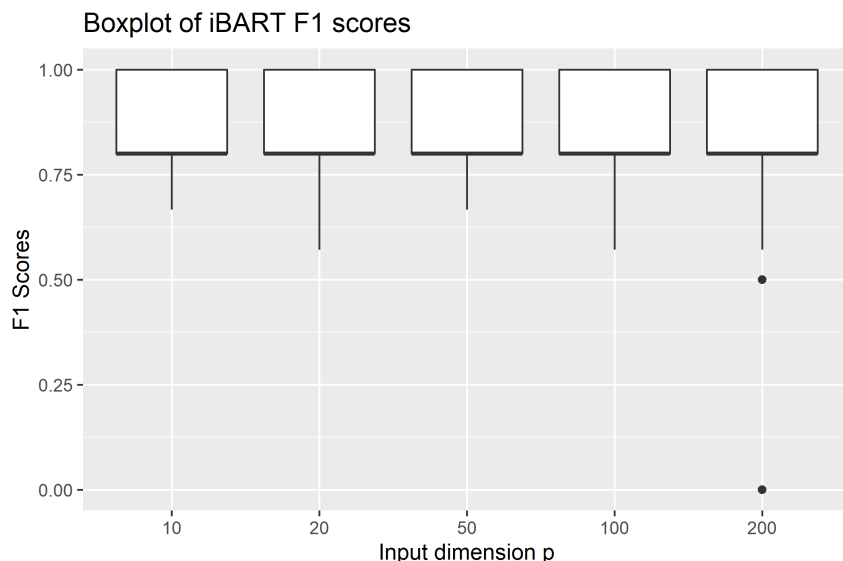


Figure 5: Boxplot of F_1 scores for iBART under Model (12) with $p \in \{10, 20, 50, 100, 200\}$.

4 Application to single-atom catalysis

We apply the proposed method to analyze a single-atom catalysis dataset (O’Connor et al., 2018) in which the goal is to identify physical descriptors that are associated with the binding energy of metal-support pairs calculated by density functional theory (DFT). Single-atom catalysts are popular in modern materials science and chemistry as they offer high reactivity and selectivity while maximizing utilization of the expensive active metal component (Yang et al., 2013; O’Connor et al., 2018; Wang et al., 2018). However, single-atom catalysts suffer from a lack of stability caused by the tendency for single metal atoms to agglomerate in a process called sintering. To prevent sintering in single-atom catalysts, one can tune the binding strength between single metal atoms and oxide supports. While first principle simulations can calculate the binding energy at given metal-support pairs, modeling their association requires explicit statistical modeling and is key to aid the design of single-atom catalysts that are robust against sintering. Feature engineering leads to physical descriptors constructed using mathematical operators and physical properties of the supported metal and the support, and gains popularity in materials informatics as the obtained descriptors are interpretable and provide insights into the underlying physical relationship. The key challenge is to select the most relevant physical properties among large-scale candidate

predictors that have explanatory and predicative power to the binding energy; often the sample size is small as first principle simulations are computationally intensive.

The data consist of $n = 91$ metal-support pairs and $p = 59$ physical properties. The binding energies of these 91 metal-support pairs are treated as a 91×1 response vector \mathbf{y} and the 59 physical properties are the primary features $\mathbf{X}_0 = (\mathbf{x}_1, \dots, \mathbf{x}_{59})$. We use the operator set given in (1) but exclude $\sin(\pi \cdot)$ and $\cos(\pi \cdot)$.

We implement iBART, SISSO, and LASSO to analyze this dataset. To enhance interpretability, we aim to find the best k descriptors for $k = 1, \dots, 5$ in this analysis. Hence, both iBART and LASSO are followed by the best subset selection with given k , corresponding to the methods of iBART+ ℓ_0 and LASSO+ ℓ_0 in Section 3.4, respectively; we suppress the notation + ℓ_0 for brevity. In the best subset selection, all candidate models contain the intercept term in addition to k descriptors. LASSO is not scalable to handle $p = 59$, and we reduce the dimension of the feature space by extensive domain knowledge, following O'Connor et al. (2018). This initial dimension reduction is not needed for SISSO or iBART. In this analysis, we eliminate non-physical descriptors such as $size + size^2$, by automatically comparing the dimensions and units of the constructed descriptors.

For iBART, we follow the settings described in Section 2.4 and identify the best k descriptors by varying the ℓ_0 -penalty parameter k up to 5. We chose the descriptor generating process (8) due to strong collinearity among the primary features; for instance, the absolute correlation between two primary features r_s^s and r_p^s is above 0.999. The SISSO parameters are set as followed. The maximum number of descriptors is set to 5; the order of composition complexity is set to 2; the maximum number of operators in a descriptor is set to 8; the absolute upper and lower bound of a descriptor is set to 1×10^8 and 1×10^{-8} , respectively; the size of the SIS-selected subspace is set to 40. We cap the order of composition complexity at 2 because the number of descriptors is already 5.5×10^7 when iteratively applying the operator set twice and applying another layer of the operator set exceeds the maximum number of elements allowed in a Fortran 90 matrix. The LASSO procedure is implemented using the MATLAB code published by O'Connor et al. (2018) on

GitHub, and all parameters are left as default.

For each method, we first calculate the out-of-sample root mean square error (RMSE). We randomly partition the $n = 91$ observations into a 90% training set (82 samples) and a 10% testing set (9 samples), and repeat this process for 50 times.

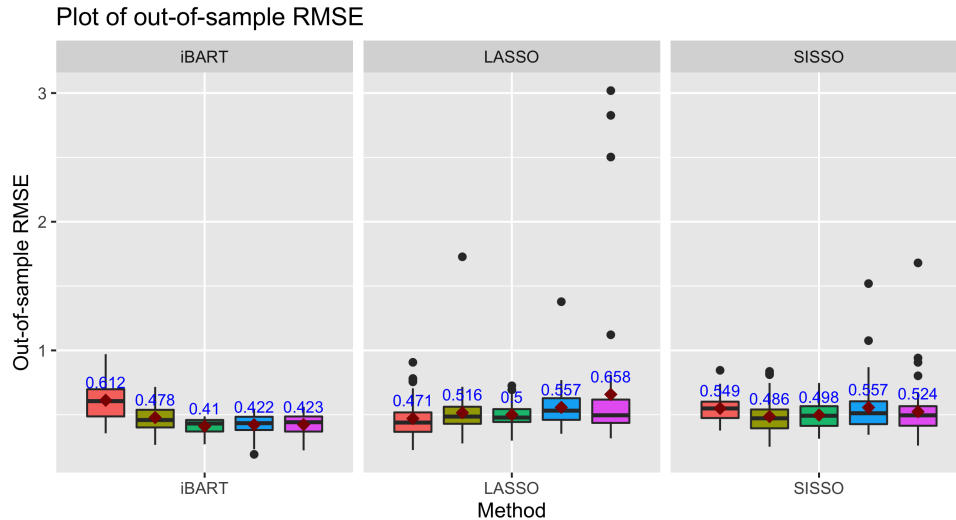


Figure 6: Boxplot of the out-of-sample RMSE for each method across 50 random partitions with $1 \leq k \leq 5$ (left to right in each plot). The blue numbers and the red rhombuses are the mean out-of-sample RMSE.

Figure 6 shows the boxplot of out-of-sample RMSE for each method. The smallest mean RMSE is attained at $k = 3$ for iBART (0.41), $k = 1$ for LASSO (0.471), and $k = 2$ for SISSO (0.486), that is, iBART reduces the RMSE by 13% relative to LASSO and 16% relative to SISSO; also see the first row of Table 1. iBART outperforms LASSO and SISSO with smaller mean RMSE and reduced variability for $k \geq 2$. LASSO gives the smallest mean RMSE when the model only contains one descriptor, that is, $k = 1$. This indicates that the predictive performance of iBART improves with more descriptors in the model. On the contrary, the RMSE of LASSO increases with more descriptors in the model, indicating overfitting. For all k , we observe iBART does not report large deviations from the mean performance, suggesting robustness to training sets compared to LASSO and SISSO.

In addition to the performance gain in out-of-sample RMSE, iBART also leads to a substantial reduction in computing time and memory usage. Table 1 shows that iBART leads to over 30-fold ($6943/225 = 30.86$) speedup compared to SISSO, and over 480-fold

($5511 \times 20/225 = 489$) speedup compared to LASSO, tested on an Intel Xeon Gold 6230 CPU @ 2.10 GHz using either 1 or 20 CPU cores. We did not obtain the accurate single-core runtime of LASSO because of its poor scalability—it is expected to take about 1530 hours ($5511 \times 20 \times 50/3600 = 1530$) to complete all 50 cross validations when run on a single core if we multiply the 20-core runtime by the number of cores. The exact speedup of iBART compared to single-core runtime of LASSO may vary due to the reduced communication cost among multiple cores and increased memory demand, but we may not expect a change in magnitude. We remark that the LASSO method implemented here is given an advantage with an additional dimension reduction step, and a full exploration of the feature space as in iBART is computationally prohibitive for LASSO. The excellent scalability of iBART transforms to memory efficiency as the descriptor space in iBART is orders of magnitude smaller than that of competing methods. Table 1 shows that iBART generates a descriptor space of size $627 < O(p^2)$ in the last iteration on average. Thanks to this significantly smaller descriptor space, we were able to run iBART on a laptop with only 16GB of memory; in contrast, LASSO and SISSO failed at the descriptor generation step owing to the enormous descriptor space they try to generate, and require server-grade computing facilities.

Table 1: Performance comparison of three methods: out-of-sample RMSE, runtime, and the number of generated descriptors, averaged over 50 cross validations.

	iBART	LASSO	SISSO
RMSE	0.41	0.471	0.486
Runtime	225 sec	5511 sec $\times 20$	6943 sec
Number of generated descriptors	627	3.3×10^5	5.5×10^7

Table 2 reports the selected descriptors by iBART with various k using the full dataset and Table 3 reports the physical meanings of the selected primary features. We can see that some descriptors are recurrent in various models, such as $\left| \frac{\Delta H_{\text{sub}} - \Delta H_{\text{f,ox,bulk}}}{\Delta E_{\text{vac}}} \right|$. This reassuringly suggests stability of the proposed descriptor selection method across k . Readers are referred to (Liu et al., 2021a) for in depth analysis and physical interpretation of these selected descriptors from the perspective of catalyst design.

The left plot in Figure 7 reports the fitting performance of the OIS model selected by

Table 2: Selected linear models by iBART for $k \in \{1, 2, 3, 4, 5\}$.

k	Selected descriptors
1	$\left \frac{\Delta H_{\text{sub}} - \Delta H_{\text{f,ox,bulk}}}{\Delta E_{\text{vac}}} \right $
2	$\frac{EA^s \cdot (\Delta H_{\text{sub}} - \Delta H_{\text{f,ox,bulk}})}{N_{\text{val}}^m / CN_{\text{bulk}}^m}, \left \frac{\Delta H_{\text{sub}} - \Delta H_{\text{f,ox,bulk}}}{\Delta E_{\text{vac}}} \right $
3	$EA^s \cdot \Delta H_{\text{f,ox,bulk}}, \left \frac{\Delta H_{\text{sub}} - \Delta H_{\text{f,ox,bulk}}}{\Delta E_{\text{vac}}} \right , \left \frac{(\eta^{1/3})^m}{N_{\text{val}}^m \cdot \Delta E_{\text{vac}}} \right $
4	$EA^s \cdot \Delta H_{\text{f,ox,bulk}}, \frac{(\eta^{1/3})^m}{\phi^s}, \frac{(\eta^{1/3})^m \cdot IE_4^s}{(N_{\text{val}}^m)^2}, \left \frac{EA^s \cdot (\Delta H_{\text{sub}} - \Delta H_{\text{f,ox,bulk}})}{\Delta E_{\text{vac}}} \right $
5	$\frac{(\eta^{1/3})^m}{\phi^s}, \frac{\Delta H_{\text{f,ox,bulk}}}{\Delta E_{\text{vac}}}, \frac{EA^s \cdot (\Delta H_{\text{sub}} - \Delta H_{\text{f,ox,bulk}})}{N_{\text{val}}^m / CN_{\text{bulk}}^m}, \frac{(\eta^{1/3})^m \cdot IE_4^s}{(N_{\text{val}}^m)^2}, \left \frac{\Delta H_{\text{sub}} - \Delta H_{\text{f,ox,bulk}}}{\Delta E_{\text{vac}}} \right $

Table 3: Descriptions of the selected primary features by iBART.

Primary feature	Physical meaning
ΔH_{sub}	Heat of sublimation
$\Delta H_{\text{f,ox,bulk}}$	Oxidation energy of the bulk metal
ΔE_{vac}	Oxygen vacancy energy
EA^s	Electron affinity of support
N_{val}^m	Valance electron of metal adatom
CN_{bulk}^m	Coordination number of the surface metal atom in the bulk phase
$(\eta^{1/3})^m$	Discontinuity in electron density of metal adatom
ϕ^s	Chemical potential of the electrons in support
IE_4^s	4th ionization energy of support with the bulk metal in the 4^+ oxidation state

iBART with three descriptors, the complexity suggested by the out-of-sample RMSE. It compares DFT binding energies predicted by the least squares estimates and the observed values. The plot centers around the black line $y = x$, suggesting model adequacy. The identified OIS model yields an R^2 of 0.9534, indicating high explanatory power. In contrast, the non-OIS model in the right plot of Figure 7, which selects the best three variables from the primary feature space \mathbf{X}_0 , shows poor fitting performance and considerable deviation from the line $y = x$. Compared to the OIS model, this model gives an $R^2 = 0.7828$, leaving 17.06% more of the variance in the response unexplained. The fitted OIS model is

$$\hat{y}_{\text{OIS}} = -0.01 + 0.40 \times (EA^s \cdot \Delta H_{\text{f,ox,bulk}}) - 0.59 \times \left| \frac{\Delta H_{\text{sub}} - \Delta H_{\text{f,ox,bulk}}}{\Delta E_{\text{vac}}} \right| - 19.63 \times \left| \frac{(\eta^{1/3})^m}{N_{\text{val}}^m \cdot \Delta E_{\text{vac}}} \right|,$$

and the fitted non-OIS model is $\hat{y}_{\text{non-OIS}} = -18.65 + 0.6098 \times IE_2^m + 0.26 \times N_{\text{val}}^s + 0.99 \times \Delta E_{\text{vac}}$. Here EA^s , $\Delta H_{\text{f,ox,bulk}}$, ΔH_{sub} , ΔE_{vac} , $(\eta^{1/3})^m$, N_{val}^m , IE_2^m and N_{val}^s are physical properties that correlate with binding energy of metal-support pair. Our application pinpoints targeted descriptors to guide further investigation into the underlying physical discovery.

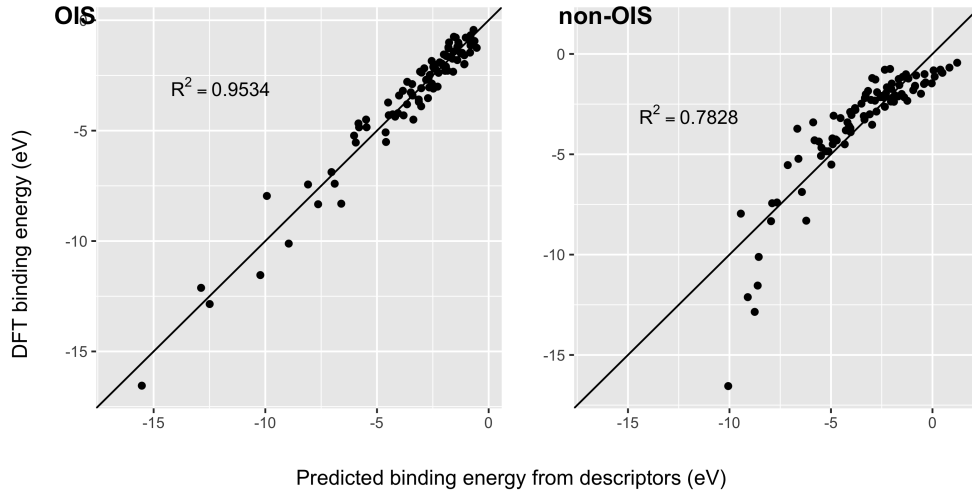


Figure 7: DFT binding energies versus predicted values using linear models with OIS and without OIS. The black line is $y = x$. Each model has $k = 3$ descriptors.

5 Discussion

In this article, we study variable selection in feature engineering that is widely applicable in many scientific fields to provide interpretable models for discovering interesting variables associated with the response. As opposed to classical variable selection, candidate predictors are engineered from primary features and composite operators. While this problem has become increasingly important in science, such as the emerging field of materials informatics, the induced new geometry has not been studied in the statistical literature. We propose a new strategy “parametrics assisted by nonparametrics”, or PAN, to efficiently explore the feature space and achieve nonparametric dimension reduction for linear models. Using BART as the nonparametric module, the proposed method iBART iteratively constructs and selects complex descriptors. Compared to one-shot descriptor construction approaches, iBART does not operate on an ultra-high dimensional descriptor space and thus substantially

mitigates the “curse of dimensionality” and high correlations among the descriptors. We introduce the OIS framework, define a desired OIS screening property, and assess BART through the lens of this property. This sets a foundation for future research in interpretable model selection with feature engineering.

Other than the methodological contributions, we use extensive experiments to demonstrate appealing empirical features of iBART that may be crucial for practitioners. iBART automates the feature generating step; one-shot methods such as LASSO often require user intervention as otherwise they are not scalable to handle the overwhelmingly large feature space—this feature space increases double exponentially in the number of primary features and operators as a result of compositions. iBART has excellent scalability and leads to robust performance when the dimension of primary features increases to a level that renders existing methods computationally infeasible. Compared to SISSO, which is widely perceived as the state-of-the-art in the field of materials genomes, our data application shows that iBART reduces the out-of-sample RMSE by 16% with an over 30-fold speedup and a fraction of memory demand. Overall, the proposed method accomplishes traditionally “server-required” tasks using a regular laptop and desktop with improved accuracy. Beyond materials genomes illustrated in Section 4, iBART can be applied to a vast domain where interpretable modeling is of interest.

There are interesting next directions building on our iBART approach. First, OIS provides a useful perspective for structured variable selection by introducing operators and compositions. Certain operator sets may be particularly useful depending on the application; for example, the composite multiply operator leads to high-order interactions. It is interesting to examine the performance of iBART with a diverse choice of operators. Also, there is a rich menu of nonparametric variable selection methods, and one may compare the performance when BART is replaced with alternatives. Finally, we have focused on finite sample performance when assessing OIS screening property through simulations partly in view of the limited sample size typically available in the motivating example. It is nevertheless interesting to theoretically investigate this property for selected nonparametric

variable selection methods such as BART when the sample size diverges.

References

- Bien, J., Taylor, J. and Tibshirani, R. (2013) A lasso for hierarchical interactions. *The Annals of Statistics*, **41**, 1111–1141.
- Bleich, J., Kapelner, A., George, E. I. and Jensen, S. T. (2014) Variable selection for BART: an application to gene regulation. *Annals of Applied Statistics*, **8**, 1750–1781.
- Chipman, H. A., George, E. I. and McCulloch, R. E. (2010) BART: Bayesian additive regression trees. *Annals of Applied Statistics*, **4**, 266–298.
- Choi, N. H., Li, W. and Zhu, J. (2010) Variable selection with the strong heredity constraint and its oracle property. *Journal of the American Statistical Association*, **105**, 354–364.
- Dor, O. and Reich, Y. (2012) Strengthening learning algorithms by feature discovery. *Information Sciences*, **189**, 176–190.
- Fan, J. and Lv, J. (2008) Sure independence screening for ultrahigh dimensional feature space. *Journal of the Royal Statistical Society: Series B (Statistical Methodology)*, **70**, 849–911.
- Feurer, M., Klein, A., Eggenberger, K., Springenberg, J., Blum, M. and Hutter, F. (2015) Efficient and robust automated machine learning. In *Advances in Neural Information Processing Systems*, vol. 28. Curran Associates, Inc.
- Foppa, L., Ghiringhelli, L. M., Girsdies, F., Hashagen, M., Kube, P., Hävecker, M., Carey, S. J., Tarasov, A., Kraus, P., Rosowski, F., Schlögl, R., Trunschke, A. and Scheffler, M. (2021) Materials genes of heterogeneous catalysis from clean experiments and artificial intelligence. *ArXiv e-prints*.
- Ghiringhelli, L. M., Vybiral, J., Levchenko, S. V., Draxl, C. and Scheffler, M. (2015) Big data of materials science: Critical role of the descriptor. *Phys. Rev. Lett.*, **114**, 105503.

- Hart, G. L., Mueller, T., Toher, C. and Curtarolo, S. (2021) Machine learning for alloys. *Nature Reviews Materials*, 1–26.
- Keith, J. A., Vassilev-Galindo, V., Cheng, B., Chmiela, S., Gastegger, M., Müller, K.-R. and Tkatchenko, A. (2021) Combining machine learning and computational chemistry for predictive insights into chemical systems. *ArXiv e-prints*.
- Khurana, U., Samulowitz, H. and Turaga, D. (2018) Feature engineering for predictive modeling using reinforcement learning. In *The Thirty-Second AAAI Conference on Artificial Intelligence (AAAI-18)*.
- Lin, Y., Saboo, A., Frey, R., Sorkin, S., Gong, J., Olson, G. B., Li, M. and Niu, C. (2021) CALPHAD uncertainty quantification and TDBX. *JOM*, **73**, 116–125.
- Liu, C.-Y., Ye, S., Li, M. and Senftle, T. P. (2021a) A rapid feature selection method for catalyst design: Iterative Bayesian Additive Regression Trees (iBART). Under review.
- Liu, C.-Y., Zhang, S., Martinez, D., Li, M. and Senftle, T. P. (2020) Using statistical learning to predict interactions between single metal atoms and modified MgO(100) supports. *npj Computational Materials*, **6**, 102.
- Liu, X., Wu, Y., Irving, D. L. and Li, M. (2021b) Gaussian graphical models with graph constraints for magnetic moment interaction in high entropy alloys. *ArXiv e-prints*.
- Markovitch, S. and Rosenstein, D. (2002) Feature generation using general constructor functions. *Machine Learning*, **49**, 59–98.
- Miller, M. J., Cabral, M. J., Dickey, E. C., LeBeau, J. M. and Reich, B. J. (2021) Accounting for location measurement error in imaging data with application to atomic resolution images of crystalline materials. *Technometrics*, **0**, 1–11.
- O’Connor, N. J., Jonayat, A. S. M., Janik, M. J. and Senftle, T. P. (2018) Interaction trends between single metal atoms and oxide supports identified with density functional theory and statistical learning. *Nature Catalysis*, **1**, 531–539.

- Ouyang, R., Curtarolo, S., Ahmetcik, E., Scheffler, M. and Ghiringhelli, L. M. (2018) SISSO: A compressed-sensing method for identifying the best low-dimensional descriptor in an immensity of offered candidates. *Physical Review Materials*, **2**, 083802.
- Radchenko, P. and James, G. M. (2010) Variable selection using adaptive nonlinear interaction structures in high dimensions. *Journal of the American Statistical Association*, **105**, 1541–1553.
- Ravikumar, P., Lafferty, J., Liu, H. and Wasserman, L. (2009) Sparse additive models. *Journal of the Royal Statistical Society: Series B (Statistical Methodology)*, **71**, 1009–1030.
- Sender, R., Fuchs, S. and Milo, R. (2016) Revised estimates for the number of human and bacteria cells in the body. *PLOS Biology*, **14**, 1–14.
- She, Y., Wang, Z. and Jiang, H. (2018) Group regularized estimation under structural hierarchy. *Journal of the American Statistical Association*, **113**, 445–454.
- Tibshirani, R. (1996) Regression shrinkage and selection via the Lasso. *Journal of the Royal Statistical Society: Series B (Methodological)*, **58**, 267–288.
- Wang, A., Li, J. and Zhang, T. (2018) Heterogeneous single-atom catalysis. *Nature Reviews Chemistry*, **2**, 65–81.
- Yang, X.-F., Wang, A., Qiao, B., Li, J., Liu, J. and Zhang, T. (2013) Single-atom catalysts: A new frontier in heterogeneous catalysis. *Accounts of Chemical Research*, **46**, 1740–1748.
- Zhong, M., Tran, K., Min, Y., Wang, C., Wang, Z., Dinh, C.-T., De Luna, P., Yu, Z., Rasouli, A. S., Brodersen, P., Sun, S., Voznyy, O., Tan, C.-S., Askerka, M., Che, F., Liu, M., Seifitokaldani, A., Pang, Y., Lo, S.-C., Ip, A., Ulissi, Z. and Sargent, E. H. (2020) Accelerated discovery of CO₂ electrocatalysts using active machine learning. *Nature*, **581**, 178–183.